Electronic Transactions on Numerical Analysis.
Volume 49, pp. 41–63, 2018.

ISSN 1068–9613.
DOI: 10.1553/etna_vol49s41

ETNA
Kent State University and
Johann Radon Institute (RICAM)

NUMERICAL ASSESSMENT OF TWO-LEVEL DOMAIN DECOMPOSITION PRECONDITIONERS FOR INCOMPRESSIBLE STOKES AND ELASTICITY EQUATIONS*

GABRIEL R. BARRENECHEA†, MICHAŁ BOSY†‡, AND VICTORITA DOLEAN†§

Abstract. Solving the linear elasticity and Stokes equations by an optimal domain decomposition method derived algebraically involves the use of non-standard interface conditions. The one-level domain decomposition preconditioners are based on the solution of local problems. This has the undesired consequence that the results are not scalable, which means that the number of iterations needed to reach convergence increases with the number of subdomains. This is the reason why in this work we introduce, and test numerically, two-level preconditioners. Such preconditioners use a coarse space in their construction. We consider the nearly incompressible elasticity problems and Stokes equations, and discretise them by using two finite element methods, namely, the hybrid discontinuous Galerkin and Taylor-Hood discretisations.

Key words. Stokes problem, nearly incompressible elasticity, Taylor-Hood, hybrid discontinuous Galerkin methods, domain decomposition, coarse space, optimized restricted additive Schwarz methods.

AMS subject classifications. 65F10, 65N22, 65N30, 65N55.

1. Introduction.

In [3], one-level domain decomposition methods for Stokes equations were introduced in conjunction with non-standard interface conditions. However, they present a lack of scalability with respect to the number of subdomains. It means that splitting the problem domain into a larger number of subdomains leads to an increase in size of the plateau region in the convergence of an iterative method (see Figure 1.1) when using the one-level domain decomposition methods. This is caused by the lack of global information, as subdomains can only communicate with their neighbours. Hence, when the number of subdomains increases in one direction, the length of the plateau also increases. Even in cases where the local problems are of the same size, the iteration count grows with the increase of the number of subdomains. This can be also observed in all the experiments in this manuscript in the case of one-level methods.

The remedy for this is the use of a second level in the preconditioner, or a coarse space correction, that adds the necessary global information. Two-level algorithms have been analysed for several classes of problems in [27]. The key point of these kind of methods is to choose an appropriate coarse space. The classical coarse space introduced by Nicolaides in [23] for a Poisson problem is defined by vectors whose support is in each subdomain, and its dimension is equal to the number of subdomains. Flow problems or linear elasticity in mixed form require a construction of a different type of coarse space as seen for example in [19]. The latter is based on a coarse grid correction and it uses the underlying properties of saddle point problems. Another type of coarse space has been introduced in [1] by using eigenvectors of local Dirichlet-to-Neumann maps. In a similar spirit, we introduce a spectral coarse space by enriching the global information to be shared by the subdomains, that generalises the classical one while allowing to attain a prescribed convergence of the two-level algorithm. As we will see in the following, this approach can help to deal with strongly heterogeneous problems. This idea was introduced for the first time in [5] in the case of multigrid methods. It relies

*Received July 26, 2017. Accepted January 9, 2018. Published online on April 20, 2018. Recommended by Marcus Sarkis.

†Department of Mathematics and Statistics, University of Strathclyde, 26 Richmond Street, G1 1XH Glasgow, United Kingdom ({Gabriel.Barrenechea,Victorita.Dolean}@strath.ac.uk).

‡Dipartimento di Matematica "F. Casorati", Università degli Studi di Pavia, Via Adolfo Ferrata 5, 27100 Pavia, Italy (Michal.Bosy@unipv.it).

§University Côte d'Azur, CNRS, LJAD, 06108 Nice Cedex 02, France.

ETNA
Kent State University and
Johann Radon Institute (RICAM)

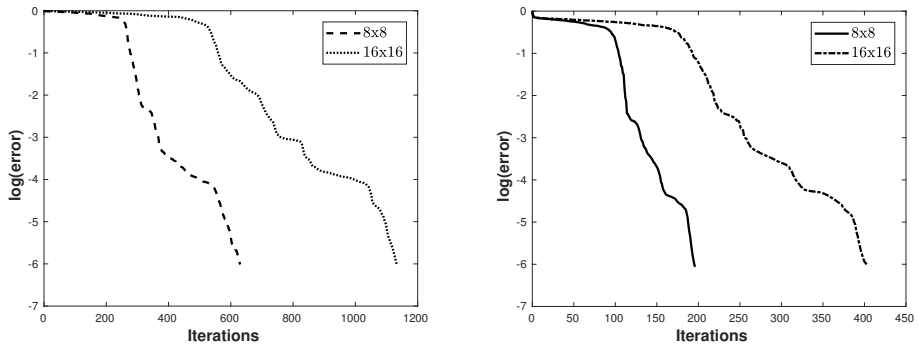

(a) Taylor-Hood (b) hdG

FIG. 1.1. *Increase in the size of the plateau region for an increasing number of subdomains.*

on solving local generalised eigenvalue problems, allowing to choose suitable vectors for the coarse space.

For overlapping domain decomposition preconditioners, a similar idea was introduced in the case of Darcy equations in [13, 14]. The authors of [22] considered also the heterogeneous Darcy equation and presented a different generalised eigenvalue problem based on local Dirichlet-to-Neumann maps. The method has been analysed in [11] and proved to be very robust in the case of small overlaps. The same idea was extended numerically to the heterogeneous Helmholtz problem in [9]. The authors of [21] apply the coarse space associated with low-frequency eigenfunctions of the subdomain Dirichlet-to-Neumann maps for the generalisation of the optimised Schwarz methods, named 2-Lagrange multiplier methods.

The first attempt to extend this spectral approach to general symmetric positive definite problems was made in [12] as an extension of [13, 14]. Since some of the assumptions of the previous framework are hard to fulfil, the authors of [26] proposed a slightly different approach for symmetric positive definite problems. Their idea of constructing a partition of unity operator associated with the degrees of freedom allows to work with various finite element spaces. An overview of different kinds of two-level methods can be found in [10, Chapters 5 and 7].

Despite the fact that all these approaches provide satisfactory results, there is no universal treatment to build efficient coarse spaces in the case of non-definite problems, such as Stokes equations. The spectral coarse spaces that we use in this work are inspired by those proposed in [16]. The authors introduced and tested numerically symmetrised two-level preconditioners for overlapping algorithms which use Robin interface conditions between the subdomains; see (5.1) for details. They have applied these preconditioners to the solution of saddle point problems, such as nearly incompressible elasticity and Stokes problems discretised by Taylor-Hood finite elements. In our case, we use non-standard interface conditions. Therefore the use of spectral coarse spaces could lead to an important gain.

In this work, we test this improvement in case of nearly incompressible elasticity and Stokes equations that are discussed in Section 2. They are discretised by the Taylor-Hood [15, Chapter II, Section 4.2] and hybrid discontinuous Galerkin methods [7, 8], presented in Section 3. In Section 4, we introduce the two-level domain decomposition preconditioners. Sections 5 and 6 present the two and three dimensional numerical experiments, respectively. Finally, a summary is outlined in Section 7.

2. The differential equations. Let Ω be an open polygon in $\mathbb{R}^2$ or an open Lipschitz polyhedron in $\mathbb{R}^3$, with Lipschitz boundary $\Gamma := \partial\Omega$. The dimension of the space is denoted by $d = 2, 3$. We use bold face letters for tensor or vector variables. In addition, we denote

ETNA
Kent State University and
Johann Radon Institute (RICAM)

the normal and tangential components as $u_n := \boldsymbol{u} \cdot \boldsymbol{n}$ and $u_t := \boldsymbol{u} - u_n \boldsymbol{n}$, where $\boldsymbol{n}$ is the outward unit normal vector to the boundary Γ .

For $D \subset \Omega$, we use the standard space $L^2(D)$ and the space $C^0(\bar{D})$, which denotes the set of all continuous functions on the closure of a set D. Let us define the following Sobolev spaces

$$\begin{aligned} H^m(D) &:= \left\{ v \in L^2(D) : \ \forall\, |\boldsymbol{\alpha}| \le m,\ \partial^{\boldsymbol{\alpha}} v \in L^2(D) \right\} \text{ for } m \in \mathbb{N}, \\ H^{\frac{1}{2}}(\partial D) &:= \left\{ \tilde{v} \in L^2(\partial D) : \ \exists v \in H^1(D),\ \tilde{v} = \mathrm{tr}(v) \right\}, \\ H(div, D) &:= \left\{ \boldsymbol{v} \in [L^2(D)]^d : \ \nabla \cdot \boldsymbol{v} \in L^2(D) \right\}, \end{aligned}$$

where, for $\boldsymbol{\alpha} = (\alpha_1, ..., \alpha_d) \in \mathbb{N}^d$ and $|\boldsymbol{\alpha}| = \sum_{i=1}^{d} \alpha_i$, we let $\partial^{\boldsymbol{\alpha}} = \frac{\partial^{|\boldsymbol{\alpha}|}}{\partial x_1^{\alpha_1} \cdots \partial x_d^{\alpha_d}}$ and $\mathrm{tr} : H^1(\Omega) \to H^{\frac{1}{2}}(\partial\Omega)$ denote the trace operator. In addition, we use the following notation for the space including boundary and average conditions

$$\begin{aligned} L_0^2(D) &:= \left\{ v \in L^2(D) : \ \int_D v \, d\boldsymbol{x} = 0 \right\}, \\ H^1_{\tilde{\Gamma}}(D) &:= \left\{ v \in H^1(D) : \ v = 0 \text{ on } \tilde{\Gamma} \right\}, \end{aligned}$$

where $\tilde{\Gamma} \subset \partial D$. If $\tilde{\Gamma} = \partial D$, then $H^1_{\tilde{\Gamma}}(D)$ is denoted as $H^1_0(D)$.

Now we present the two differential problems considered in this work.

2.1. Stokes equation. Let us start with the d-dimensional ($d = 2, 3$) Stokes problem

$$\begin{cases} -\nu \Delta \boldsymbol{u} + \nabla p = \boldsymbol{f}, & \text{in } \Omega, \\ \nabla \cdot \boldsymbol{u} = 0, & \text{in } \Omega, \end{cases} \tag{2.1}$$

where $\boldsymbol{u} : \bar{\Omega} \to \mathbb{R}^d$ is the velocity field, $p : \bar{\Omega} \to \mathbb{R}$ the pressure, $\nu > 0$ the viscosity, which is considered to be constant, and $\boldsymbol{f} \in [L^2(\Omega)]^d$ is a given function. We define the stress tensor $\boldsymbol{\sigma} := \nu \nabla \boldsymbol{u} - p\boldsymbol{I}$ and the flux as $\boldsymbol{\sigma_n} := \boldsymbol{\sigma}\, \boldsymbol{n}$. For $\boldsymbol{u_D} \in [H^{\frac{1}{2}}(\Gamma)]^d$ and $g \in L^2(\Gamma)$ we consider three types of boundary conditions:

- Dirichlet (non-slip)

$$\boldsymbol{u} = \boldsymbol{u_D} \text{ on } \Gamma; \tag{2.2}$$

- tangential-velocity and normal-flux (TVNF)

$$\begin{cases} u_t = 0, & \text{on } \Gamma, \\ \sigma_{nn} = g, & \text{on } \Gamma; \end{cases} \tag{2.3}$$

- normal-velocity and tangential-flux (NVTF)

$$\begin{cases} u_n = 0, & \text{on } \Gamma, \\ \sigma_{nt} = g, & \text{on } \Gamma. \end{cases} \tag{2.4}$$

The third type of boundary condition has already been considered for the Stokes problem in [2].

ETNA
Kent State University and
Johann Radon Institute (RICAM)

2.2. Nearly incompressible elasticity equation. From a mathematical point of view, the nearly incompressible elasticity problem is very similar to the Stokes equations. The difference is that instead of considering the gradient $\nabla \boldsymbol{v}$, the symmetric gradient $\boldsymbol{\varepsilon}(\boldsymbol{v}) := \frac{1}{2}\left(\nabla \boldsymbol{v} + \nabla^T \boldsymbol{v}\right)$ is used. We want to solve the following d-dimensional ($d = 2, 3$) problem

$$\begin{cases} -2\mu \nabla \cdot \boldsymbol{\varepsilon}(\boldsymbol{u}) + \nabla p = \boldsymbol{f}, & \text{in } \Omega, \\ -\nabla \cdot \boldsymbol{u} = \frac{1}{\lambda} p, & \text{in } \Omega, \end{cases} \tag{2.5}$$

where $\boldsymbol{u} : \bar{\Omega} \to \mathbb{R}^d$ is the displacement field, $p : \Omega \to \mathbb{R}$ the pressure, $\boldsymbol{f} \in [L^2(\Omega)]^d$ is a given function, λ and μ are the Lamé coefficients, defined by

$$\lambda = \frac{E\nu}{(1+\nu)(1-2\nu)}, \qquad \mu = \frac{E}{2(1+\nu)},$$

where E is the Young modulus and ν the Poisson ratio. We define the stress tensor as $\boldsymbol{\sigma}^{\text{sym}} := 2\mu\boldsymbol{\varepsilon}(\boldsymbol{u}) - p\boldsymbol{I}$ and its normal component as $\boldsymbol{\sigma}_{\boldsymbol{n}}^{\text{sym}} := \boldsymbol{\sigma}^{\text{sym}}\boldsymbol{n}$. For $g \in L^2(\Gamma)$ we consider three types of boundary conditions:

- mixed: for $\Gamma = \Gamma_D \cup \Gamma_N$ with $\Gamma_D \cap \Gamma_N = \emptyset$, we impose

$$\begin{cases} \boldsymbol{u} = 0, & \text{on } \Gamma_D, \\ \boldsymbol{\sigma}_{\boldsymbol{n}}^{\text{sym}} = 0, & \text{on } \Gamma_N; \end{cases} \tag{2.6}$$

- tangential-displacement and normal-normal-stress (TDNNS)

$$\begin{cases} u_t = 0, & \text{on } \Gamma, \\ \sigma_{nn}^{\text{sym}} = g, & \text{on } \Gamma; \end{cases} \tag{2.7}$$

- normal-displacement and tangential-normal-stress (NDTNS)

$$\begin{cases} u_n = 0, & \text{on } \Gamma, \\ \sigma_{nt}^{\text{sym}} = g, & \text{on } \Gamma. \end{cases} \tag{2.8}$$

The second type of boundary condition has already been considered for linear elasticity equation in [24].

3. The numerical methods. Let $\{\mathcal{T}_h\}_{h>0}$ be a regular family of triangulations of $\bar{\Omega}$ made of simplices. For each triangulation $\mathcal{T}_h$, $\mathcal{E}_h$ denotes the set of its facets (edges for $d = 2$, faces for $d = 3$). In addition, for each element $K \in \mathcal{T}_h$, $h_K := \text{diam}(K)$, and we set $h := \max_{K \in \mathcal{T}_h} h_K$. We define the following broken Sobolev spaces on the set of all edges in $\mathcal{E}_h$ (for $d = 2$)

$$L^2(\mathcal{E}_h) := \left\{ v : \ v|_E \in L^2(E), \ \forall\, E \in \mathcal{E}_h \right\}.$$

Moreover, for $D \subset \Omega$, $\mathbb{P}_k(D)$ denotes the space of polynomials of total degree smaller than (or equal to) k on the set D.

We now present the two discretisations that will be used in the numerical experiments.

3.1. Taylor-Hood discretisation. We first consider the Taylor-Hood discretisation using the following approximation spaces

$$\boldsymbol{TH}_{\boldsymbol{h}}^{\boldsymbol{k}} := \left\{ \boldsymbol{v_h} \in [H^1(\Omega)]^d : \ \boldsymbol{v_h}|_K \in [\mathbb{P}_k(K)]^d, \ \forall\, K \in \mathcal{T}_h \right\},$$
$$R_h^{k-1} := \left\{ q_h \in C^0(\bar{\Omega}) : \ q_h|_K \in \mathbb{P}_{k-1}(K), \ \forall\, K \in \mathcal{T}_h \right\},$$

ETNA
Kent State University and
Johann Radon Institute (RICAM)

where $k \geq 2$; see [15, Chapter II, Section 4.2].

If (2.1) is supplied with the homogeneous boundary conditions (2.2), then the discrete problem reads:

Find $(\boldsymbol{u_h}, p_h) \in \left(\boldsymbol{TH_h^k} \cap [H_0^1(\Omega)]^d\right) \times \left(R_h^{k-1} \cap L_0^2(\Omega)\right)$
s.t. for all $(\boldsymbol{v_h}, q_h) \in \left(\boldsymbol{TH_h^k} \cap [H_0^1(\Omega)]^d\right) \times \left(R_h^{k-1} \cap L_0^2(\Omega)\right)$

$$\begin{cases} \displaystyle\int_\Omega \nu \nabla \boldsymbol{u_h} : \nabla \boldsymbol{v_h}\, d\boldsymbol{x} - \int_\Omega p_h \nabla \cdot \boldsymbol{v_h}\, d\boldsymbol{x} &= \displaystyle\int_\Omega \boldsymbol{f}\boldsymbol{v_h}\, d\boldsymbol{x}, \\ \displaystyle -\int_\Omega \nabla \cdot \boldsymbol{u_h} q_h\, d\boldsymbol{x} &= 0. \end{cases}$$

In case of TVNF boundary conditions (2.3), we define $\boldsymbol{V_t} := \left\{\boldsymbol{v} \in [H^1(\Omega)]^d : \ v_t = 0 \text{ on } \Gamma\right\}$, and the discrete problem reads:

Find $(\boldsymbol{u_h}, p_h) \in \left(\boldsymbol{TH_h^k} \cap \boldsymbol{V_t}\right) \times R_h^{k-1}$
s.t. for all $(\boldsymbol{v_h}, q_h) \in \left(\boldsymbol{TH_h^k} \cap \boldsymbol{V_t}\right) \times R_h^{k-1}$

$$\begin{cases} \displaystyle\int_\Omega \nu \nabla \boldsymbol{u_h} : \nabla \boldsymbol{v_h}\, d\boldsymbol{x} - \int_\Omega p_h \nabla \cdot \boldsymbol{v_h}\, d\boldsymbol{x} &= \displaystyle\int_\Omega \boldsymbol{f}\boldsymbol{v_h}\, d\boldsymbol{x} + \int_\Gamma g\, (\boldsymbol{v_h})_t\ ds, \\ \displaystyle -\int_\Omega \nabla \cdot \boldsymbol{u_h} q_h\, d\boldsymbol{x} &= 0. \end{cases} \tag{3.1}$$

If NVTF boundary conditions (2.4) are used, then we define the space

$$\boldsymbol{V_n} := \left\{\boldsymbol{v} \in [H^1(\Omega)]^d : \ v_n = 0 \text{ on } \Gamma\right\},$$

and the discrete problem reads:

Find $(\boldsymbol{u_h}, p_h) \in \left(\boldsymbol{TH_h^k} \cap \boldsymbol{V_n}\right) \times \left(R_h^{k-1} \cap L_0^2(\Omega)\right)$
s.t. for all $(\boldsymbol{v_h}, q_h) \in \left(\boldsymbol{TH_h^k} \cap \boldsymbol{V_n}\right) \times \left(R_h^{k-1} \cap L_0^2(\Omega)\right)$

$$\begin{cases} \displaystyle\int_\Omega \nu \nabla \boldsymbol{u_h} : \nabla \boldsymbol{v_h}\, d\boldsymbol{x} - \int_\Omega p_h \nabla \cdot \boldsymbol{v_h}\, d\boldsymbol{x} &= \displaystyle\int_\Omega \boldsymbol{f}\boldsymbol{v_h}\, d\boldsymbol{x} + \int_\Gamma g\, (\boldsymbol{v_h})_n\ ds, \\ \displaystyle -\int_\Omega \nabla \cdot \boldsymbol{u_h} q_h\, d\boldsymbol{x} &= 0. \end{cases} \tag{3.2}$$

In a similar way, if the problem (2.5) is supplied with the boundary conditions (2.6), then the discrete problem reads

Find $(\boldsymbol{u_h}, p_h) \in \left(\boldsymbol{TH_h^k} \cap [H_{\Gamma_D}^1(\Omega)]^d\right) \times R_h^{k-1}$
s.t. for all $(\boldsymbol{v_h}, q_h) \in \left(\boldsymbol{TH_h^k} \cap [H_{\Gamma_D}^1(\Omega)]^d\right) \times R_h^{k-1}$

$$\begin{cases} \displaystyle\int_\Omega 2\mu \boldsymbol{\varepsilon}\left(\boldsymbol{u_h}\right) : \boldsymbol{\varepsilon}\left(\boldsymbol{v_h}\right)\, d\boldsymbol{x} - \int_\Omega p_h \nabla \cdot \boldsymbol{v_h}\, d\boldsymbol{x} &= \displaystyle\int_\Omega \boldsymbol{f}\boldsymbol{v_h}\, d\boldsymbol{x}, \\ \displaystyle -\int_\Omega \nabla \cdot \boldsymbol{u_h} q_h\, d\boldsymbol{x} - \frac{1}{\lambda}\int_\Omega p_h q_h\, d\boldsymbol{x} &= 0. \end{cases}$$

The other discrete problems associated with (2.5), equipped with either TDNNS boundary conditions (2.7) or NDTNS boundary conditions (2.8), are similar to (3.1) or (3.2), respectively.

ETNA
Kent State University and
Johann Radon Institute (RICAM)

3.2. Hybrid discontinuous Galerkin discretisation. We restrict the discussion to the two dimensional case $d = 2$. This method has been presented and analysed in [3]. The velocity is approximated using the Brezzi-Douglas-Marini spaces (see [4, Section 2.3.1]) of degree k given by

$$\boldsymbol{BDM}_{\boldsymbol{h}}^{\boldsymbol{k}} := \left\{ \boldsymbol{v_h} \in H(div,\Omega) : \ \boldsymbol{v_h}|_K \in \left[\mathbb{P}_k\left(K\right)\right]^2, \ \forall K \in \mathcal{T}_h \right\},$$
$$\boldsymbol{BDM}_{\boldsymbol{h},\tilde{\boldsymbol{\Gamma}}}^{\boldsymbol{k}} := \left\{ \boldsymbol{v_h} \in H(div,\Omega) : \ \boldsymbol{v_h}|_K \in \left[\mathbb{P}_k\left(K\right)\right]^2, \ \forall K \in \mathcal{T}_h, \ \left(\boldsymbol{v_h}\right)_n = 0 \text{ on } \tilde{\Gamma} \right\},$$

where $\tilde{\Gamma} \subset \partial\Omega$. If $\tilde{\Gamma} = \partial\Omega$, then $\boldsymbol{BDM}_{\boldsymbol{h},\tilde{\boldsymbol{\Gamma}}}^{\boldsymbol{k}}$ is denoted $\boldsymbol{BDM}_{\boldsymbol{h},\boldsymbol{0}}^{\boldsymbol{k}}$.

The pressure is approximated in the space

$$Q_h^{k-1} := \left\{ q_h \in L^2\left(\Omega\right) : \ q_h|_K \in \mathbb{P}_{k-1}\left(K\right), \ \forall K \in \mathcal{T}_h \right\}.$$

Finally, we introduce a Lagrange multiplier, aimed at approximating the tangential component of the velocity. The space where this multiplier is sought is given by

$$M_h^{k-1} := \left\{ \tilde{v}_h \in L^2\left(\mathcal{E}_h\right) : \ \tilde{v}_h|_E \in \mathbb{P}_{k-1}\left(E\right), \ \forall E \in \mathcal{E}_h \right\},$$
$$M_{h,\tilde{\Gamma}}^{k-1} := \left\{ \tilde{v}_h \in M_h^{k-1} : \tilde{v}_h = 0 \text{ on } \tilde{\Gamma} \right\},$$

where $\tilde{\Gamma} \subset \partial\Omega$. The latter space incorporates some boundary conditions and, if $\tilde{\Gamma} = \partial\Omega$, then $M_{h,\tilde{\Gamma}}^{k-1}$ is denoted $M_{h,0}^{k-1}$. Furthermore, we introduce for all $E \in \mathcal{E}_h$ the $L^2(E)$-projection $\Phi_E^{k-1} : L^2\left(E\right) \to \mathbb{P}_{k-1}\left(E\right)$, defined by

$$\int_E \Phi_E^{k-1}(\tilde{w})\tilde{v}_h \, ds = \int_E \tilde{w}\tilde{v}_h \, ds, \quad \forall \tilde{v}_h \in \mathbb{P}_{k-1}\left(E\right),$$

and we set $\Phi^{k-1} : L^2\left(\mathcal{E}_h\right) \to M_h^{k-1}$, defined as $\Phi^{k-1}|_E := \Phi_E^{k-1}$ for all $E \in \mathcal{E}_h$.

If (2.1) is supplied with the homogeneous boundary conditions (2.2), then the discrete problem reads:

Find $(\boldsymbol{u_h}, \tilde{u}_h, p_h) \in \boldsymbol{BDM}_{\boldsymbol{h},\boldsymbol{0}}^{\boldsymbol{k}} \times M_{h,0}^{k-1} \times \left(Q_h^{k-1} \cap L_0^2(\Omega)\right)$
s.t. for all $(\boldsymbol{v_h}, \tilde{v}_h, q_h) \in \boldsymbol{BDM}_{\boldsymbol{h},\boldsymbol{0}}^{\boldsymbol{k}} \times M_{h,0}^{k-1} \times \left(Q_h^{k-1} \cap L_0^2(\Omega)\right)$,

$$\begin{cases} a\left((\boldsymbol{u_h}, \tilde{u}_h), (\boldsymbol{v_h}, \tilde{v}_h)\right) + b\left((\boldsymbol{v_h}, \tilde{v}_h), p_h\right) &= \displaystyle\int_\Omega \boldsymbol{f}\boldsymbol{v_h} \, d\boldsymbol{x}, \\ b\left((\boldsymbol{u_h}, \tilde{u}_h), q_h\right) &= 0, \end{cases}$$

where

$$\begin{aligned} a\left((\boldsymbol{w_h}, \tilde{w}_h), (\boldsymbol{v_h}, \tilde{v}_h)\right) := \sum_{K \in \mathcal{T}_h} \Bigg(& \int_K \nu \nabla \boldsymbol{w_h} : \nabla \boldsymbol{v_h} \, d\boldsymbol{x} \\ & - \int_{\partial K} \nu \left(\boldsymbol{\partial_n} \boldsymbol{w_h}\right)_t \left(\left(\boldsymbol{v_h}\right)_t - \tilde{v}_h \right) ds \\ & - \int_{\partial K} \nu \left(\left(\boldsymbol{w_h}\right)_t - \tilde{w}_h \right) \left(\boldsymbol{\partial_n} \boldsymbol{v_h}\right)_t \, ds \\ & + \nu \frac{\tau}{h_K} \int_{\partial K} \Phi^{k-1}\left(\left(\boldsymbol{w_h}\right)_t - \tilde{w}_h \right) \Phi^{k-1}\left(\left(\boldsymbol{v_h}\right)_t - \tilde{v}_h \right) ds \Bigg), \end{aligned}$$

ETNA
Kent State University and
Johann Radon Institute (RICAM)

$\tau > 0$ is a stabilisation parameter, and

$$b\left(\left(\boldsymbol{v_h}, \tilde{v}_h\right), q_h\right) := -\sum_{K \in \mathcal{T}_h} \int_K q_h \nabla \cdot \boldsymbol{v_h} \, d\boldsymbol{x}. \tag{3.3}$$

If TVNF boundary conditions (2.3) are used, then the discrete problem reads:

Find $(\boldsymbol{u_h}, \tilde{u}_h, p_h) \in \boldsymbol{BDM_h^k} \times M_{h,0}^{k-1} \times Q_h^{k-1}$
s.t. for all $(\boldsymbol{v_h}, \tilde{v}_h, q_h) \in \boldsymbol{BDM_h^k} \times M_{h,0}^{k-1} \times Q_h^{k-1}$,

$$\begin{cases} a\left(\left(\boldsymbol{u_h}, \tilde{u}_h\right), \left(\boldsymbol{v_h}, \tilde{v}_h\right)\right) + b\left(\left(\boldsymbol{v_h}, \tilde{v}_h\right), p_h\right) & = \displaystyle\int_\Omega \boldsymbol{f v_h} \, d\boldsymbol{x} + \int_\Gamma g \left(\boldsymbol{v_h}\right)_n \, ds, \\ b\left(\left(\boldsymbol{u_h}, \tilde{u}_h\right), q_h\right) & = 0. \end{cases} \tag{3.4}$$

In case of NVTF boundary conditions (2.4), the discrete problem reads:

Find $(\boldsymbol{u_h}, \tilde{u}_h, p_h) \in \boldsymbol{BDM_{h,0}^k} \times M_h^{k-1} \times \left(Q_h^{k-1} \cap L_0^2(\Omega)\right)$
s.t. for all $(\boldsymbol{v_h}, \tilde{v}_h, q_h) \in \boldsymbol{BDM_{h,0}^k} \times M_h^{k-1} \times \left(Q_h^{k-1} \cap L_0^2(\Omega)\right)$,

$$\begin{cases} a\left(\left(\boldsymbol{u_h}, \tilde{u}_h\right), \left(\boldsymbol{v_h}, \tilde{v}_h\right)\right) + b\left(\left(\boldsymbol{v_h}, \tilde{v}_h\right), p_h\right) & = \displaystyle\int_\Omega \boldsymbol{f v_h} \, d\boldsymbol{x} + \int_\Gamma g \tilde{v}_h \, ds, \\ b\left(\left(\boldsymbol{u_h}, \tilde{u}_h\right), q_h\right) & = 0. \end{cases} \tag{3.5}$$

In a similar way, if the problem (2.5) is supplied with the mixed boundary conditions (2.6), then the discrete problem reads:

Find $(\boldsymbol{u_h}, \tilde{u}_h, p_h) \in \boldsymbol{BDM_{h,\Gamma_D}^k} \times M_{h,\Gamma_D}^{k-1} \times Q_h^{k-1}$
s.t. for all $(\boldsymbol{v_h}, \tilde{v}_h, q_h) \in \boldsymbol{BDM_{h,\Gamma_D}^k} \times M_{h,\Gamma_D}^{k-1} \times Q_h^{k-1}$,

$$\begin{cases} a_s\left(\left(\boldsymbol{u_h}, \tilde{u}_h\right), \left(\boldsymbol{v_h}, \tilde{v}_h\right)\right) + b\left(\left(\boldsymbol{v_h}, \tilde{v}_h\right), p_h\right) & = \displaystyle\int_\Omega \boldsymbol{f v_h} \, d\boldsymbol{x}, \\ b\left(\left(\boldsymbol{u_h}, \tilde{u}_h\right), q_h\right) + c(p_h, q_h) & = 0, \end{cases}$$

where

$$\begin{aligned} a_s\left(\left(\boldsymbol{w_h}, \tilde{w}_h\right), \left(\boldsymbol{v_h}, \tilde{v}_h\right)\right) := \sum_{K \in \mathcal{T}_h} \Bigg(& \int_K 2\mu \boldsymbol{\varepsilon}(\boldsymbol{w_h}) : \boldsymbol{\varepsilon}(\boldsymbol{v_h}) \, d\boldsymbol{x} \\ & - \int_{\partial K} 2\mu \left(\boldsymbol{\varepsilon_n}(\boldsymbol{w_h})\right)_t \left(\left(\boldsymbol{v_h}\right)_t - \tilde{v}_h\right) ds \\ & - \int_{\partial K} 2\mu \left(\left(\boldsymbol{w_h}\right)_t - \tilde{w}_h\right) \left(\boldsymbol{\varepsilon_n}(\boldsymbol{v_h})\right)_t \, ds \\ & + 2\mu \frac{\tau}{h_K} \int_{\partial K} \Phi^{k-1}\left(\left(\boldsymbol{w_h}\right)_t - \tilde{w}_h\right) \Phi^{k-1}\left(\left(\boldsymbol{v_h}\right)_t - \tilde{v}_h\right) ds \Bigg), \end{aligned}$$

b is defined by (3.3), and

$$c(r_h, q_h) := -\frac{1}{\lambda} \int_\Omega r_h q_h \, ds.$$

The other discrete problems associated with (2.5), equipped with either TDNNS boundary conditions (2.7) or NDTNS boundary conditions (2.8), are similar to (3.4) or (3.5), respectively.

ETNA
Kent State University and
Johann Radon Institute (RICAM)

4. The domain decomposition preconditioners. Let us assume that we have to solve the following linear system $\mathbf{A}\boldsymbol{U} = \boldsymbol{F}$, where $\mathbf{A}$ is the matrix arising from the discretisation of the Stokes or linear elasticity equation on the domain Ω, $\boldsymbol{U}$ is the vector of unknowns, and $\boldsymbol{F}$ is the right-hand side. To accelerate the performance of an iterative Krylov method [10, Chapter 3] applied to this system, we will consider domain decomposition preconditioners which are naturally parallel. They are based on an overlapping decomposition of the computational domain.

(a) L-shaped domain (b) T-shaped domain

FIG. 4.1. *Partition of the domain for 8 subdomains by METIS.*

Let $\{\mathcal{T}_{h,i}\}_{i=1}^N$ be a partition of the triangulation $\mathcal{T}_h$; see examples in Figure 4.1. For an integer value $l \geq 0$, we set $\mathcal{T}_{h,i}^0 = \mathcal{T}_{h,i}$ and define an overlapping decomposition $\{\mathcal{T}_{h,i}^l\}_{i=1}^N$ such that $\mathcal{T}_{h,i}^l$ is a set of all triangles from $\mathcal{T}_{h,i}^{l-1}$ and all triangles from $\mathcal{T}_h \setminus \mathcal{T}_{h,i}^{l-1}$ that have non-empty intersection with $\mathcal{T}_{h,i}^{l-1}$. With this definition, the width of the overlap will be $2l$. Furthermore, if W_h stands for the finite element space associated to $\mathcal{T}_h$, let $W_{h,i}^l$ be the local finite element space on $\mathcal{T}_{h,i}^l$, which is a triangulation of Ω_i.

Let $\mathcal{N}$ be the set of indices of degrees of freedom of W_h and $\mathcal{N}_i^l$ the set of indices of degrees of freedom of $W_{h,i}^l$ for $l \geq 0$. Moreover, we define the restriction operator $\mathbf{R}_i : W_h \to W_{h,i}^l$ as a rectangular matrix of size $|\mathcal{N}_i^l| \times |\mathcal{N}|$, such that if $\boldsymbol{V}$ is the vector of degrees of freedom of $v_h \in W_h$, then $\mathbf{R}_i\boldsymbol{V}$ is the vector of degrees of freedom of $W_{h,i}^l$ in Ω_i. The extension operator from $W_{h,i}^l$ to W_h and its associated matrix are both given by $\mathbf{R}_i^T$. In addition, we introduce a partition of the unity $\mathbf{D}_i$ as a diagonal matrix of size $|\mathcal{N}_i^l| \times |\mathcal{N}_i^l|$, such that

$$\mathbf{Id} = \sum_{i=1}^N \mathbf{R}_i^T \mathbf{D}_i \mathbf{R}_i,$$

where $\mathbf{Id} \in \mathbb{R}^{|\mathcal{N}| \times |\mathcal{N}|}$ is the identity matrix.

We first recall the Modified Restricted Additive Schwarz (MRAS) preconditioner introduced in [3] for the Stokes equation. This preconditioner is given by

$$\mathbf{M}_{MRAS}^{-1} = \sum_{i=1}^N \mathbf{R}_i^T \mathbf{D}_i \mathbf{B}_i^{-1} \mathbf{R}_i, \tag{4.1}$$

ETNA
Kent State University and
Johann Radon Institute (RICAM)

where $\mathbf{B}_i$ is the matrix associated to a discretisation of the Stokes equation (2.1) in Ω_i where we impose either TVNF (2.3) or NVTF (2.4) boundary conditions on $\partial\Omega_i \cap \Omega$. In the case of a discretisation of the elasticity equation (2.5) in Ω_i, we impose either TDNNS (2.7) or NDTNS (2.8) boundary conditions on $\partial\Omega_i \cap \Omega$.

We now introduce a symmetrised variant of (4.1), called Symmetrised Modified Restricted Additive Schwarz (SMRAS), given by

$$\mathbf{M}_{SMRAS}^{-1} = \sum_{i=1}^{N} \mathbf{R}_i^T \mathbf{D}_i \mathbf{B}_i^{-1} \mathbf{D}_i \mathbf{R}_i. \tag{4.2}$$

4.1. Two-level methods. A two-level version of the SMRAS and MRAS preconditioners will be based on a spectral coarse space obtained by solving the following local generalised eigenvalue problems

Find $(\boldsymbol{V}_{jk}, \lambda_{jk}) \in (\mathbb{R}^{|\mathcal{N}_j|} \setminus \{0\}) \times \mathbb{R}$ *s.t.*

$$\tilde{\mathbf{A}}_j \boldsymbol{V}_{jk} = \lambda_{jk} \mathbf{B}_j \boldsymbol{V}_{jk}\,. \tag{4.3}$$

Here, the $\tilde{\mathbf{A}}_j$ are local matrices associated to a discretisation of a local Neumann boundary value problem in Ω_j, where the Neumann boundary conditions are imposed only on the interface between the subdomains and not on the physical boundary. For example, in the case of the Stokes problem (2.1) with Dirichlet boundary conditions (2.2), we consider the following local problem

$$\begin{cases} -\nu\Delta \boldsymbol{u} + \nabla p &= \boldsymbol{f}, & \text{in } \Omega_j, \\ \nabla \cdot \boldsymbol{u} &= 0, & \text{in } \Omega_j, \\ \boldsymbol{u} &= \boldsymbol{u_D}, & \text{on } \Gamma, \\ \boldsymbol{\sigma_n} &= 0, & \text{on } \partial\Omega_j \setminus \Gamma. \end{cases}$$

Let $\theta > 0$ be a user-defined threshold. We define $Z_{GenEO} \subset \mathbb{R}^{|\mathcal{N}|}$ as the vector space spanned by the family of vectors $\left(\mathbf{R}_j^T \mathbf{D}_j \boldsymbol{V}_{jk}\right)_{\lambda_{jk}<\theta}$, $1 \leq j \leq N$, corresponding to eigenvalues smaller than θ. The value of θ is chosen such that, for a given problem and preconditioner, the behaviour of the method is robust, in the sense that its convergence does not depend, or depends very weakly, on the number of subdomains.

We are now ready to introduce the two-level method with coarse space Z_{GenEO}. Let $\mathbf{P}_0$ be the $\mathbf{A}$-orthogonal projection onto the coarse space Z_{GenEO}. The two-level SMRAS preconditioner is defined as

$$\mathbf{M}_{SMRAS,2}^{-1} = \mathbf{P}_0 \mathbf{A}^{-1} + (\mathbf{Id} - \mathbf{P}_0)\mathbf{M}_{SMRAS}^{-1}(\mathbf{Id} - \mathbf{P}_0^T).$$

Furthermore, if $\mathbf{R}_0$ is a matrix whose rows are a basis for the coarse space Z_{GenEO}, then

$$\mathbf{P}_0 \mathbf{A}^{-1} = \mathbf{R}_0^T \left(\mathbf{R}_0 \mathbf{A} \mathbf{R}_0^T\right)^{-1} \mathbf{R}_0.$$

In a similar way, we can introduce the two-level MRAS preconditioner

$$\mathbf{M}_{MRAS,2}^{-1} = \mathbf{P}_0 \mathbf{A}^{-1} + (\mathbf{Id} - \mathbf{P}_0)\mathbf{M}_{MRAS}^{-1}(\mathbf{Id} - \mathbf{P}_0^T).$$

ETNA
Kent State University and
Johann Radon Institute (RICAM)

5. Numerical results for two dimensional problems. In this section we assess the performance of the preconditioners defined in Section 4.1. We compare the newly introduced ones with that of ORAS and SORAS, introduced in [16]. This kind of preconditioners are associated with the Robin interface conditions and require an optimised parameter, as it can be seen in (5.1) below. The big advantage of the SMRAS and MRAS preconditioners from the previous section is that they are parameter-free. We consider the partial differential equation model for nearly incompressible elasticity and Stokes flow as problems of similar mixed formulation. Each of these problems is discretised by using the Taylor-Hood method from Section 3.1 and the hdG discretisation from Section 3.2.

Our experiments are based on the classical weak scaling test. This test is built as follows. A domain $\bar{\Omega}$ is split into a triangulation $\mathcal{T}_h$. For each of element $K \in \mathcal{T}_h$, $h_K = \text{diam}(K)$, and we denote the mesh size by $h := \max_{K\in\mathcal{T}_h} h_K$. Then, this triangulation is split into overlapping subdomains of size H, in such a way that $\frac{H}{h}$ remains constant. In the absence of a second level in the preconditioner, if the number of subdomains grows then the convergence gets slower. A coarse space provides global information and leads to more robust behaviour.

The simplest way to build a coarse space is to consider the zero energy modes. More precisely, they are the eigenvectors associated with the zero eigenvalues of (4.3) on a floating subdomains. Here, by a floating subdomain we mean a subdomain without Dirichlet boundary condition on any part of the boundary. Then the matrix on the left-hand side of (4.3) is singular and there are zero eigenvalues. These zero energy modes are the rigid body motions (three in two dimensions, six in three dimensions) for the elasticity problem, and the constants (two in two dimensions, three in three dimensions) for the Stokes equations. Unfortunately, for some cases this choice is not sufficient, so we have collected the smallest M eigenvalues for each subdomain and build a coarse space by including the eigenvectors associated to them. The different values of M are presented in the table in brackets.

All experiments have been made by using FreeFem++ [17], which is a free software specialised in variational discretisations of partial differential equations. We use GMRES [25] as an iterative solver. Generalized eigenvalue problems to generate the coarse space are solved using ARPACK [20]. The overlapping decomposition into subdomains can be uniform (Unif) or generated by METIS (MTS) [18]. In each of the examples, we consider decompositions with two layers of mesh size h in the overlap. Tables show the number of iterations needed to achieve a relative l^2-norm of the error smaller than 10^{-6}, that is, $\frac{\|\boldsymbol{U}-\boldsymbol{U}_n\|_{l^2}}{\|\boldsymbol{U}-\boldsymbol{U}_0\|_{l^2}} < 10^{-6}$, where $\boldsymbol{U}$ is the solution of the global problem produced by a direct solver, and $\boldsymbol{U}_m$ denotes the mth iteration of the iterative solver. In addition, DOF stands for number of degrees of freedom and N for the number of subdomains in all tables.

5.1. Taylor-Hood discretisation. In this section we consider the Taylor-Hood discretisation from Section 3.1, with different values of $k \geq 2$ for nearly incompressible elasticity and Stokes equations.

5.1.1. Nearly incompressible elasticity. Since we consider the preconditioners with various interface conditions, we need to comment the way of imposing them. ORAS and SORAS preconditioners follow [16] and use Robin interface conditions. This means that the weak formulation of the linear elasticity problem contains the following term

$$\int_{\partial\Omega_i\setminus\Gamma} \boldsymbol{\sigma}_{\boldsymbol{n}}^{\text{sym}}(\boldsymbol{v_h})_n \, ds + \int_{\partial\Omega_i\setminus\Gamma} 2\alpha\frac{\mu(2\mu+\lambda)}{\lambda+3\mu}\boldsymbol{u_h}\boldsymbol{v_h} \, ds, \tag{5.1}$$

where again, following [16], we choose $\alpha = 10$. Fortunately, the MRAS and SMRAS preconditioners are parameter-free. In this section, for all the associated numerical experiments

ETNA
Kent State University and
Johann Radon Institute (RICAM)

we use the zero vector as an initial guess for the GMRES iterative solver. Moreover, the overlapping decomposition into subdomains is generated by METIS.

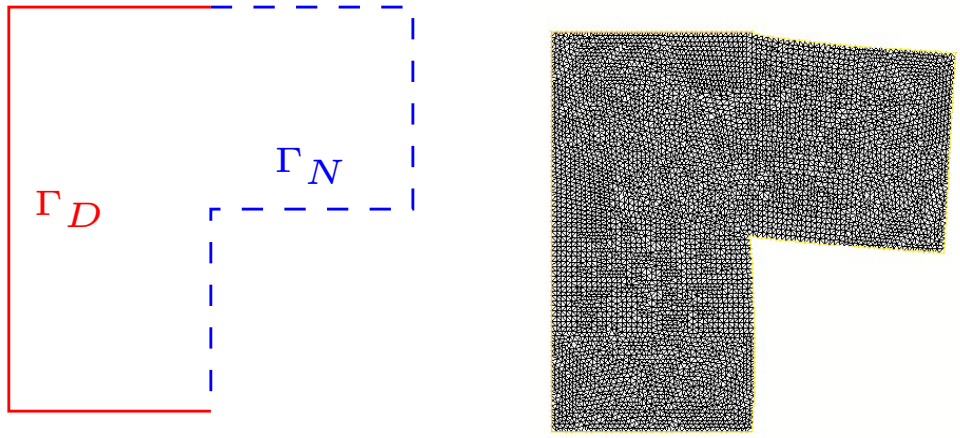

(a) Domain and boundary

(b) Discrete solution

FIG. 5.1. *L-shaped domain problem.*

TEST CASE 5.1 (The L-shaped domain problem). We consider the L-shaped domain $\Omega = (-1,1)^2 \setminus \{(0,1) \times (-1,0)\}$ clamped on the left side and partly from the top and the bottom, as depicted in Figure 5.1(a). This example is similar to the one in [6]. The associated boundary value problem is

$$\left\{\begin{array}{rcrcll} -2\mu\nabla\cdot\boldsymbol{\varepsilon}(\boldsymbol{u}) & + & \nabla p & = & (0,-1)^T, & \text{in } \Omega, \\ & - & \nabla\cdot\boldsymbol{u} & = & \frac{1}{\lambda}p, & \text{in } \Omega, \\ & & \boldsymbol{u}(x,y) & = & (0,0)^T, & \text{on } \Gamma_D, \\ & & \boldsymbol{\sigma}_{\boldsymbol{n}}^{\text{sym}}(x,y) & = & (0,0)^T, & \text{on } \Gamma_N. \end{array}\right. \tag{5.2}$$

The physical parameters are $E = 10^5$ and $\nu = 0.4999$, hence the problem is nearly incompressible. In Figure 5.1(b) we plot the mesh of the bent domain.

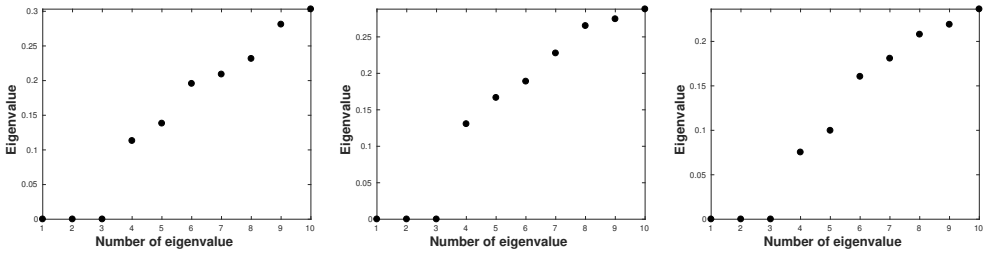

(a) Robin interface conditions

(b) NDTNS interface conditions

(c) TDNNS interface conditions

FIG. 5.2. *Eigenvalues on one of the floating subdomains in case of uniform decomposition and Taylor-Hood discretisation ($\boldsymbol{TH}_{\boldsymbol{h}}^{\boldsymbol{3}}$, R_h^2)—the L-shaped domain problem.*

We choose $k = 3$ for the Taylor-Hood discretisation. In Figure 5.2 we plot the eigenvalues of one floating subdomain. The clustering of small eigenvalues of the generalised eigenvalue

ETNA
Kent State University and
Johann Radon Institute (RICAM)

problem defined in (4.3) suggests the number of eigenvectors to be added to the coarse space. The three zero eigenvalues correspond to the zero energy modes.

TABLE 5.1
Comparison of preconditioners for Taylor-Hood discretisation ($\boldsymbol{TH}^{\mathbf{3}}_{\boldsymbol{h}}$, R^2_h) - the L-shaped domain problem.

		One-level					
DOF	N	ORAS	SORAS	NDTNS-MRAS	NDTNS-SMRAS	TDNNS-MRAS	TDNNS-SMRAS
124 109	4	26	60	26	60	30	59
478 027	16	57	131	69	143	65	140
933 087	32	84	180	109	221	104	211
1 899 125	64	130	293	181	362	161	312
3 750 823	128	209	412	302	568	251	510
		Two-level (3 eigenvectors)					
DOF	N	ORAS	SORAS	NDTNS-MRAS	NDTNS-SMRAS	TDNNS-MRAS	TDNNS-SMRAS
124 109	4	18	40	19	36	24	41
478 027	16	37	52	40	57	46	56
933 087	32	49	57	56	67	53	66
1 899 125	64	65	64	70	75	61	74
3 750 823	128	83	64	74	77	75	72
		Two-level (5 eigenvectors)					
DOF	N	ORAS	SORAS	NDTNS-MRAS	NDTNS-SMRAS	TDNNS-MRAS	TDNNS-SMRAS
124 109	4	15	32	17	35	24	37
478 027	16	31	41	31	47	42	47
933 087	32	40	48	38	52	53	51
1 899 125	64	49	51	45	53	64	56
3 750 823	128	69	54	49	54	70	53
		Two-level (7 eigenvectors)					
DOF	N	ORAS	SORAS	NDTNS-MRAS	NDTNS-SMRAS	TDNNS-MRAS	TDNNS-SMRAS
124 109	4	14	33	16	30	24	35
478 027	16	26	41	25	38	42	44
933 087	32	31	43	25	42	49	46
1 899 125	64	39	47	30	39	59	50
3 750 823	128	58	49	30	43	61	50

The results of Table 5.1 show a clear improvement in the scalability of the two-level preconditioners over the one-level ones. In fact, using five eigenvectors per subdomain, the number of iterations is virtually unaffected by the number of subdomains. All two-level preconditioners show a comparable performance. For this case, increasing the dimension of the coarse space beyond $5 \times N$ eigenvectors does not seem to improve the results dramatically.

TEST CASE 5.2 (The heterogeneous beam problem). We consider a heterogeneous beam with ten layers of steel and rubber. Five layers are made from steel, with the physical parameters $E = 210 \cdot 10^9$ and $\nu = 0.3$, and five are made from rubber, with the physical parameters $E = 10^8$ and $\nu = 0.4999$, as depicted in Figure 5.3(a). A similar example was considered in [16]. The computational domain is the rectangle $\Omega = (0, 5) \times (0, 1)$. The beam

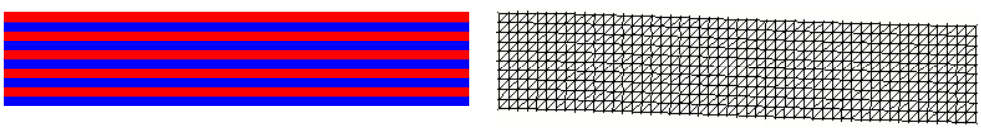

(a) Steel and rubber layers

(b) Discrete solution

FIG. 5.3. *Heterogeneous beam.*

ETNA
Kent State University and
Johann Radon Institute (RICAM)

is clamped on its left side, hence we consider the following problem

$$
\left\{
\begin{array}{rcccll}
-2\mu\nabla\cdot\boldsymbol{\varepsilon}(\boldsymbol{u}) & + & \nabla p & = & (0,-1)^T, & \text{in } \Omega,\\
 & - & \nabla\cdot\boldsymbol{u} & = & \frac{1}{\lambda}p, & \text{in } \Omega,\\
 & & \boldsymbol{u}(x,y) & = & (0,0)^T, & \text{on } \partial\Omega\cap\{x=0\},\\
 & & \boldsymbol{\sigma}_{\boldsymbol{n}}^{\text{sym}}(x,y) & = & (0,0)^T, & \text{on } \partial\Omega\setminus\{x=0\}.
\end{array}
\right. \tag{5.3}
$$

In Figure 5.3(b) we plot the mesh of the bent beam. Because of the heterogeneity of the problem, we do not notice a clear clustering of the eigenvalues; see Figure 5.4. In such case, it is well-known that a coarse space including only three zero energy modes is not sufficient [11]. That is why we consider a coarse space built using 5 or 7 eigenvectors per subdomain.

TABLE 5.2
Comparison of preconditioners for Taylor-Hood discretisation ($\boldsymbol{TH_h^3}$, R_h^2)—the heterogeneous beam.

		One-level					
DOF	N	ORAS	SORAS	NDTNS-MRAS	NDTNS-SMRAS	TDNNS-MRAS	TDNNS-SMRAS
44 963	8	168	301	160	267	177	264
87 587	16	226	490	245	462	229	424
177 923	32	373	711	447	684	440	672
347 651	64	615	>1000	728	>1000	746	>1000
707 843	128	973	>1000	>1000	>1000	>1000	>1000
1 385 219	256	>1000	>1000	>1000	>1000	>1000	>1000
		Two-level (5 eigenvectors)					
DOF	N	ORAS	SORAS	NDTNS-MRAS	NDTNS-SMRAS	TDNNS-MRAS	TDNNS-SMRAS
44 963	8	109	160	136	147	148	136
87 587	16	136	204	192	200	181	184
177 923	32	193	291	296	275	326	276
347 651	64	260	304	363	282	491	299
707 843	128	412	356	420	369	601	346
1 385 219	256	379	414	448	400	711	317
		Two-level (7 eigenvectors)					
DOF	N	ORAS	SORAS	NDTNS-MRAS	NDTNS-SMRAS	TDNNS-MRAS	TDNNS-SMRAS
44 963	8	76	118	124	115	133	103
87 587	16	106	146	166	138	159	123
177 923	32	157	202	203	185	302	214
347 651	64	178	191	225	170	326	182
707 843	128	140	114	153	112	266	122
1 385 219	256	119	86	118	77	259	94

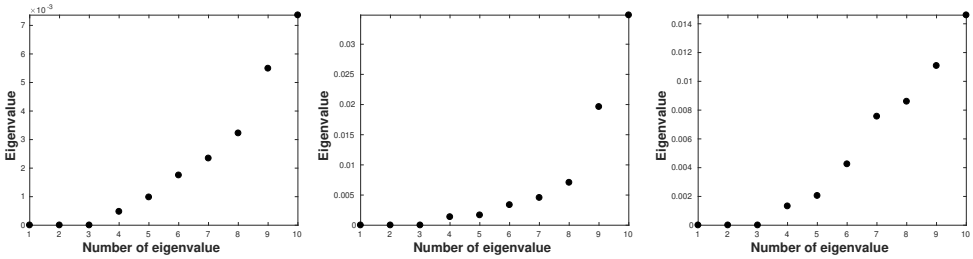

(a) Robin interface conditions (b) NDTNS interface conditions (c) TDNNS interface conditions

FIG. 5.4. *Eigenvalues on one of the floating subdomains in case of METIS decomposition and Taylor-Hood discretisation ($\boldsymbol{TH_h^3}$, R_h^2)—the heterogeneous beam.*

As in the previous example, the introduction of a coarse space provides a significant improvement in the number of iterations needed for convergence. Due to the high heterogeneity

ETNA
Kent State University and
Johann Radon Institute (RICAM)

of this problem, more eigenvectors per subdomain are needed to obtain scalable results. We notice an important improvement of the convergence when using two-level methods (see Table 5.2), although we get a stable number of iterations only when considering a coarse space which is sufficiently big.

5.1.2. Stokes equation. We now turn to the Stokes discrete problem given in Sections 3.1. Once again in case of ORAS and SORAS we choose $\alpha = 10$ as in [16] for the Robin interface conditions (5.1). In the first case we consider a random initial guess for the GMRES iterative solver. Later, with the second example, we will use the zero vector as initial guess.

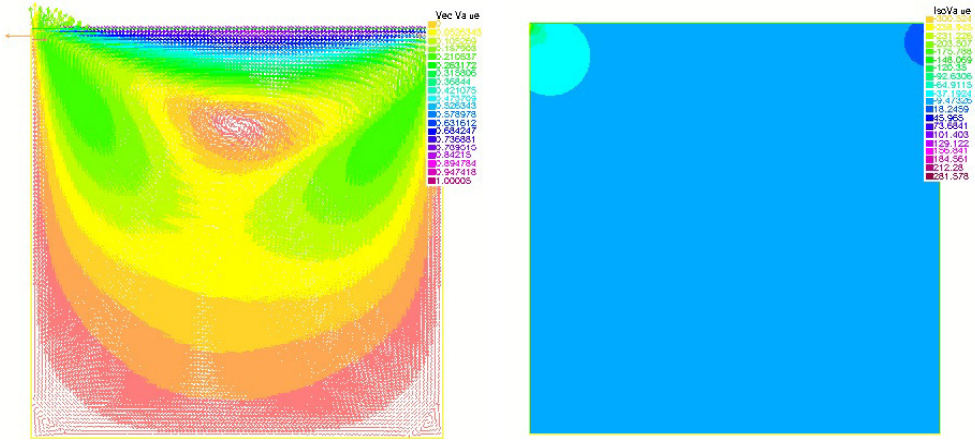

(a) Velocity field (b) Pressure

FIG. 5.5. *Numerical solution of the driven cavity problem.*

TEST CASE 5.3 (The driven cavity problem). We consider the following problem on the unit square $\Omega = (0,1)^2$

$$\left\{\begin{array}{rcrcll} -\Delta \boldsymbol{u} & + & \nabla p & = & \boldsymbol{f}, & \text{in } \Omega, \\ & - & \nabla \cdot \boldsymbol{u} & = & 0, & \text{in } \Omega, \\ & & \boldsymbol{u}(x,y) & = & (1,0)^T, & \text{on } \partial\Omega \cap \{y=1\}, \\ & & \boldsymbol{u}(x,y) & = & (0,0)^T, & \text{on } \partial\Omega \setminus \{y=1\}. \end{array}\right. \tag{5.4}$$

In Figure 5.5 we depict the discrete velocity and pressure.

We start with two energy modes only; see Figure 5.6. This already provides some improvement. Then, we add more eigenvectors to see if they bring a further improvement.

The conclusions remain the same as for the L-shaped domain problem for the nearly incompressible elasticity equation discretised by Taylor-Hood method $(\boldsymbol{TH_h^3}, R_h^2)$, since Tables 5.3 and 5.1 show similar results.

TEST CASE 5.4 (The T-shaped domain problem). Finally, we consider a T-shaped domain $\Omega = (0,1.5)\times(0,1) \cup (0.5,1)\times(-1,1)$, and we impose Dirichlet boundary conditions given by

$$\boldsymbol{u}(x,y) = \begin{cases} (4y(1-y),0)^T, & \text{if } x = 0 \text{ or } x = 1.5, \\ (0,0)^T, & \text{otherwise.} \end{cases} \tag{5.5}$$

The numerical solution of this problem is depicted in Figure 5.7. The overlapping decomposition into subdomains is generated by METIS.

ETNA
Kent State University and
Johann Radon Institute (RICAM)

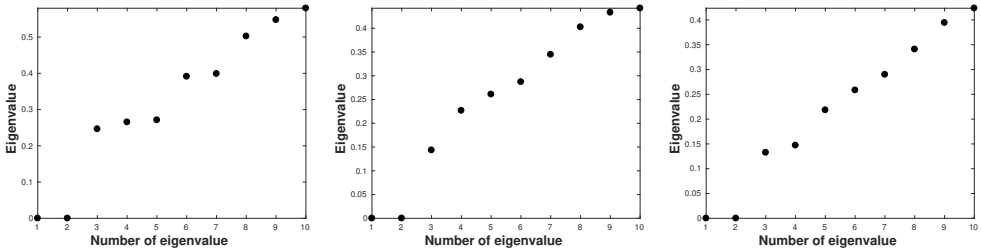

(a) [Robin interface conditions (b) NVTF interface conditions (c) VNF interface conditions]

FIG. 5.6. *Eigenvalues on one of the floating subdomains in case of uniform decomposition and Taylor-Hood discretisation ($\boldsymbol{TH^2_h}$, R^1_h)—the driven cavity problem.*

TABLE 5.3
Comparison of preconditioners for Taylor-Hood discretisation ($\boldsymbol{TH^2_h}$, R^1_h)—the driven cavity problem.

		One-level											
DOF	N	ORAS		SORAS		NVTF-MRAS		NVTF-SMRAS		TVNF-MRAS		TVNF-SMRAS	
		Unif	MTS	Unif	MTS	Unif	MTS	Unif	MTS	Unif	MTS	Unif	MTS
91 003	4	12	17	24	34	22	22	34	40	22	25	30	40
362 003	16	28	35	56	67	52	53	90	106	54	53	70	84
813 003	36	39	75	92	103	85	91	165	185	91	88	118	136
1 444 003	64	53	91	120	144	120	135	254	283	132	132	169	206
2 728 003	121	80	278	180	212	182	280	412	580	199	213	251	439
5 768 003	256	>1000	>1000	271	317	303	452	917	955	322	319	397	695
		Two-level (2 eigenvectors)											
DOF	N	ORAS		SORAS		NVTF-MRAS		NVTF-SMRAS		TVNF-MRAS		TVNF-SMRAS	
		Unif	MTS	Unif	MTS	Unif	MTS	Unif	MTS	Unif	MTS	Unif	MTS
91 003	4	10	14	18	22	19	17	26	30	27	20	21	26
362 003	16	20	25	32	37	33	34	50	62	60	40	42	51
813 003	36	27	33	36	44	47	49	62	86	79	53	59	63
1 444 003	64	31	42	38	53	104	66	85	114	85	52	62	79
2 728 003	121	39	103	39	51	74	81	85	133	92	86	62	93
5 768 003	256	300	849	46	54	109	108	146	132	91	78	63	90
		Two-level (5 eigenvectors)											
DOF	N	ORAS		SORAS		NVTF-MRAS		NVTF-SMRAS		TVNF-MRAS		TVNF-SMRAS	
		Unif	MTS	Unif	MTS	Unif	MTS	Unif	MTS	Unif	MTS	Unif	MTS
91 003	4	9	12	13	16	16	15	18	20	25	20	16	18
362 003	16	16	20	21	24	27	22	28	37	56	37	26	35
813 003	36	23	27	25	26	33	30	39	40	65	41	28	37
1 444 003	64	26	36	27	29	40	34	35	45	77	45	28	42
2 728 003	121	35	41	29	32	43	38	34	48	84	72	29	47
5 768 003	256	66	60	32	33	56	41	60	49	88	61	29	44

Once again a clustering of small eigenvalues of generalised eigenvalue problem defined in (4.3) is a motivation of the size of the coarse space; see Figure 5.8.

As in all examples for Taylor-Hood discretisation, we notice an important improvement in the convergence when two-level methods are used, although from Table 5.4 we can see that the coarse spaces containing five eigenvectors seem to be sufficient.

5.2. hdG discretisation. In this section we discretise the nearly incompressible elasticity equation and the Stokes flow by using the lowest order hdG discretisation ($k = 1$) introduced in Section 3.2.

5.2.1. Nearly incompressible elasticity. In case of ORAS and SORAS we consider the Robin interface conditions as in [16], with $\alpha = 10$. For all numerical experiments in this

ETNA
Kent State University and
Johann Radon Institute (RICAM)

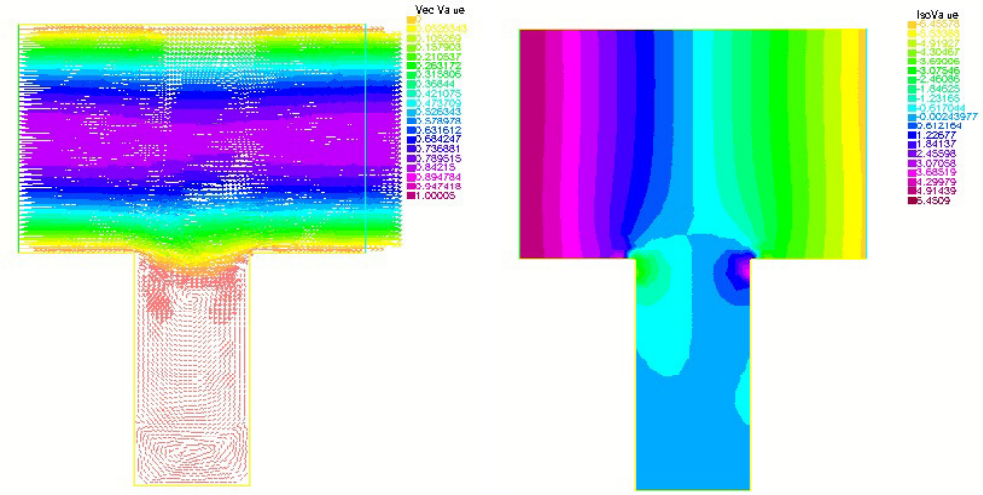

Velocity field $\boldsymbol{u}$ (b) Pressure p

FIG. 5.7. *Numerical solution—the T-shaped problem.*

TABLE 5.4
Comparison of preconditioners for Taylor-Hood discretisation ($\boldsymbol{TH_h^3}$, R_h^2)—the T-shaped problem.

		One-level					
DOF	N	ORAS	SORAS	NVTF-MRAS	NVTF-SMRAS	TVNF-MRAS	TVNF-SMRAS
33 269	4	13	20	12	19	13	19
138 316	16	36	51	33	52	31	45
269 567	32	59	85	52	85	49	75
553 103	64	92	132	83	136	78	115
1 134 314	128	146	208	132	223	117	188
2 201 908	256	232	328	209	357	189	293
		Two-level (2 eigenvectors)					
DOF	N	ORAS	SORAS	NVTF-MRAS	NVTF-SMRAS	TVNF-MRAS	TVNF-SMRAS
33 269	4	10	14	9	15	12	15
138 316	16	21	27	19	24	22	24
269 567	32	29	35	30	38	25	30
553 103	64	35	45	34	43	33	35
1 134 314	128	42	52	47	58	34	41
2 201 908	256	47	56	69	76	38	45
		Two-level (5 eigenvectors)					
DOF	N	ORAS	SORAS	NVTF-MRAS	NVTF-SMRAS	TVNF-MRAS	TVNF-SMRAS
33 269	4	8	13	8	13	12	14
138 316	16	15	16	14	16	20	18
269 567	32	14	19	20	22	24	19
553 103	64	16	20	18	19	29	20
1 134 314	128	17	22	23	24	30	22
2 201 908	256	16	21	34	37	35	24

section we use the zero vector as an initial guess for the GMRES iterative solver. Moreover, the overlapping decomposition into subdomains is generated by METIS.

TEST CASE 5.5 (The L-shaped domain problem). We consider the L-shaped domain for the discrete problem (5.2).

ETNA
Kent State University and
Johann Radon Institute (RICAM)

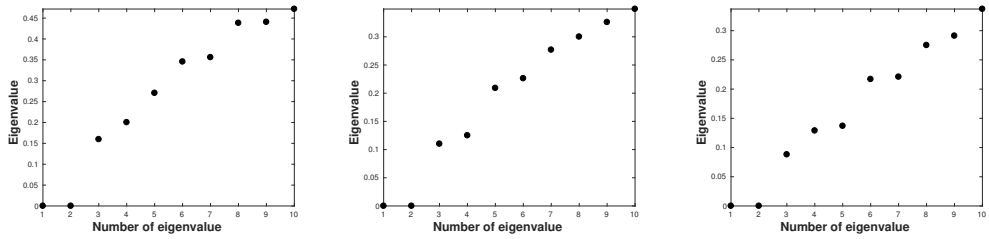

(a) Robin interface conditions (b) NVTF interface conditions (c) [TVNF interface conditions

FIG. 5.8. *Eigenvalues on one of the floating subdomains in case of METIS decomposition and Taylor-Hood discretisation ($\boldsymbol{TH_h^3}$, R_h^2)—the T-shaped problem.*

TABLE 5.5
Comparison of preconditioners for hdG discretisation—the L-shaped domain problem.

		One-level					
DOF	N	ORAS	SORAS	NDTNS-MRAS	NDTNS-SMRAS	TDNNS-MRAS	TDNNS-SMRAS
238 692	8	61	158	64	174	77	177
466 094	16	123	232	101	259	109	306
948 921	32	267	331	160	415	179	473
1 874 514	64	622	477	243	685	254	657
3 856 425	128	>1000	752	479	>1000	523	>1000
		Two-level (3 eigenvectors)					
DOF	N	ORAS	SORAS	NDTNS-MRAS	NDTNS-SMRAS	TDNNS-MRAS	TDNNS-SMRAS
238 692	8	48	98	52	98	61	116
466 094	16	89	99	71	123	75	148
948 921	32	250	130	110	158	118	173
1 874 514	64	535	135	135	155	129	159
3 856 425	128	>1000	152	172	176	181	192
		Two-level (5 eigenvectors)					
DOF	N	ORAS	SORAS	NDTNS-MRAS	NDTNS-SMRAS	TDNNS-MRAS	TDNNS-SMRAS
238 692	8	43	81	44	74	61	94
466 094	16	77	82	51	92	63	103
948 921	32	197	100	79	119	96	121
1 874 514	64	429	103	102	122	110	138
3 856 425	128	>1000	118	122	129	141	167
		Two-level (7 eigenvectors)					
DOF	N	ORAS	SORAS	NDTNS-MRAS	NDTNS-SMRAS	TDNNS-MRAS	TDNNS-SMRAS
238 692	8	35	67	38	71	44	82
466 094	16	61	79	47	80	51	95
948 921	32	153	90	58	95	74	115
1 874 514	64	423	95	71	93	72	111
3 856 425	128	934	110	79	104	108	133

Table 5.5 shows an important improvement in the convergence that is brought by the two-level methods. We cannot conclude that SMRAS preconditioners are much better than SORAS, although we can note that coarse space improvement is visible for MRAS preconditioners and not for ORAS. For symmetric preconditioners (SMRAS and SORAS), five eigenvectors seem to lead already to satisfactory results, while for the non-symmetric ones a bigger coarse space is required. On the other hand, we state the fact that the new preconditioners are parameter-free, which makes them easier to use.

TEST CASE 5.6 (The heterogeneous beam problem). We consider the heterogeneous beam with ten layers of steel and rubber defined as in the problem (5.3).

We notice an improvement only when using a coarse space that is sufficiently large; see Table 5.6. Furthermore, we get a stable number of iterations only for the symmetric

ETNA
Kent State University and
Johann Radon Institute (RICAM)

TABLE 5.6
Comparison of preconditioners for hdG discretisation—the heterogeneous beam.

		One-level					
DOF	N	ORAS	SORAS	NDTNS-MRAS	NDTNS-SMRAS	TDNNS-MRAS	TDNNS-SMRAS
46 777	8	196	440	189	402	186	463
88 720	16	317	602	330	582	326	666
179 721	32	537	>1000	574	>1000	587	>1000
353 440	64	899	>1000	847	>1000	846	>1000
704 329	128	>1000	>1000	>1000	>1000	>1000	>1000
1 410 880	256	>1000	>1000	>1000	>1000	>1000	>1000
		Two-level (5 eigenvectors)					
DOF	N	ORAS	SORAS	NDTNS-MRAS	NDTNS-SMRAS	TDNNS-MRAS	TDNNS-SMRAS
46 777	8	168	255	162	230	161	275
88 720	16	244	313	273	299	262	346
179 721	32	385	525	442	458	469	587
353 440	64	514	444	551	526	590	558
704 329	128	835	557	782	684	765	832
1 410 880	256	>1000	567	>1000	694	844	821
		Two-level (7 eigenvectors)					
DOF	N	ORAS	SORAS	NDTNS-MRAS	NDTNS-SMRAS	TDNNS-MRAS	TDNNS-SMRAS
46 777	8	148	197	149	192	158	231
88 720	16	205	201	286	187	283	273
179 721	32	318	337	385	301	433	419
353 440	64	403	262	397	247	460	389
704 329	128	490	168	447	182	558	443
1 410 880	256	>1000	116	387	138	473	298

preconditioners (SMRAS and SORAS), and the coarse space improvement in case of ORAS preconditioner is much less visible than in case of MRAS preconditioners. This may be due to the fact we have not chosen an optimized parameter in the Robin interface conditions (5.1).

5.2.2. The Stokes equation. We now turn to the Stokes discrete problem given in Section 3.2. Once again in case of ORAS and SORAS we choose $\alpha = 10$ as in [16] for the Robin interface conditions (5.1). In the first case, we consider a random initial guess for the GMRES iterative solver. Later, with the second example, we will use the zero vector as initial guess.

TEST CASE 5.7 (The driven cavity problem). We consider the driven cavity defined as in the problem (5.4). The conclusions remain the same as in the case of the nearly incompressible elasticity equation for the L-shaped domain, although Table 5.7 shows that the coarse spaces containing five eigenvectors seem to decrease the number of iterations even in the case of MRAS preconditioners that are not fully scalable.

TEST CASE 5.8 (The T-shaped domain problem). Finally, we consider a T-shaped domain $\Omega = (0, 1.5) \times (0, 1) \cup (0.5, 1) \times (-1, 1)$, and we impose mixed boundary conditions (5.5). The numerical solution of this problem is depicted in Figure 5.7.

In this case, scalable results can only be observed for the preconditioners associated with the non-standard interface conditions (MRAS and SMRAS), and when using a coarse space that is sufficiently large; see Table 5.8. In the case of ORAS or SORAS, one possibility is to choose a different parameter α, but the proof of this, as well as the question of whether this would have a positive impact, are open problems.

6. Numerical results for three dimensional problems. In this section we again assess the performance of the preconditioners as in Section 5, but this time in case of three dimensional problems. We consider the three-dimensional analogues of the Stokes and nearly incompressible elasticity problems considered in last section. Both problems are discretised

ETNA
Kent State University and
Johann Radon Institute (RICAM)

TABLE 5.7
Comparison of preconditioners for hdG discretisation—the driven cavity problem.

		One-level											
DOF	N	ORAS		SORAS		NVTF-MRAS		NVTF-SMRAS		TVNF-MRAS		TVNF-SMRAS	
		Unif	MTS	Unif	MTS	Unif	MTS	Unif	MTS	Unif	MTS	Unif	MTS
93 656	4	17	18	37	38	24	22	44	44	32	25	48	50
373 520	16	76	122	75	84	52	54	107	111	68	67	122	126
839 592	36	152	327	120	133	91	96	194	200	112	115	206	210
1 491 872	64	261	587	162	176	130	143	294	303	159	158	292	286
2 819 432	121	364	>1000	229	256	199	213	504	649	238	251	628	643
5 963 072	256	592	>1000	367	398	326	477	>1000	>1000	392	404	995	740
		Two-level (2 eigenvectors)											
DOF	N	ORAS		SORAS		NVTF-MRAS		NVTF-SMRAS		TVNF-MRAS		TVNF-SMRAS	
		Unif	MTS	Unif	MTS	Unif	MTS	Unif	MTS	Unif	MTS	Unif	MTS
93 656	4	12	14	30	28	18	18	33	32	40	23	38	37
373 520	16	81	80	47	57	36	40	61	73	100	49	85	82
839 592	36	236	228	61	60	57	65	97	104	132	66	112	107
1 491 872	64	395	463	67	71	79	85	139	129	142	70	128	122
2 819 432	121	840	>1000	73	86	113	127	188	178	157	86	127	139
5 963 072	256	>1000	>1000	80	87	171	179	283	287	167	108	132	148
		Two-level (5 eigenvectors)											
DOF	N	ORAS		SORAS		NVTF-MRAS		NVTF-SMRAS		TVNF-MRAS		TVNF-SMRAS	
		Unif	MTS	Unif	MTS	Unif	MTS	Unif	MTS	Unif	MTS	Unif	MTS
93 656	4	10	12	25	24	14	16	23	22	52	22	29	26
373 520	16	27	35	38	37	27	29	38	41	117	39	53	53
839 592	36	135	84	45	41	35	37	51	50	145	49	64	61
1 491 872	64	278	212	49	45	44	42	58	55	157	59	64	64
2 819 432	121	607	584	56	49	46	56	58	62	162	81	65	75
5 963 072	256	>1000	>1000	62	55	52	64	57	69	166	75	65	75

TABLE 5.8
Comparison of preconditioners for hdG discretisation—the T-shaped problem.

		One-level					
DOF	N	ORAS	SORAS	NVTF-MRAS	NVTF-SMRAS	TVNF-MRAS	TVNF-SMRAS
38 803	4	22	45	36	49	22	51
154 606	16	111	98	83	172	83	182
311 369	32	265	144	133	262	130	266
616 772	64	568	238	212	410	195	412
1 246 136	128	>1000	494	333	665	313	602
2 451 365	256	>1000	712	464	>1000	477	889
		Two-level (2 eigenvectors)					
DOF	N	ORAS	SORAS	NVTF-MRAS	NVTF-SMRAS	TVNF-MRAS	TVNF-SMRAS
38 803	4	16	35	31	37	21	38
154 606	16	113	69	73	75	38	75
311 369	32	254	99	103	176	93	162
616 772	64	510	153	171	273	121	140
1 246 136	128	>1000	221	242	252	155	138
2 451 365	256	>1000	286	343	515	189	231
		Two-level (5 eigenvectors)					
DOF	N	ORAS	SORAS	NVTF-MRAS	NVTF-SMRAS	TVNF-MRAS	TVNF-SMRAS
38 803	4	14	30	27	27	28	30
154 606	16	155	54	54	45	25	44
311 369	32	159	55	72	59	29	52
616 772	64	426	88	106	83	37	76
1 246 136	128	955	113	115	99	43	72
2 451 365	256	>1000	182	138	101	54	73

ETNA
Kent State University and
Johann Radon Institute (RICAM)

by using the Taylor-Hood methods from Section 3.1. In addition, we use the same tools as in Section 5. For both test cases we use the zero vector as initial guess.

6.1. Taylor-Hood discretisation. In this section we consider the Taylor-Hood discretisation from Section 3.1, with $k = 2$, for nearly incompressible elasticity and Stokes equations.

6.1.1. Nearly incompressible elasticity. In the three dimensional space, ORAS and SORAS preconditioners also require an optimized parameter. We follow [16] and use Robin interface conditions (5.1) with $\alpha = 10$.

TEST CASE 6.1 (The homogeneous beam problem). We consider a homogeneous beam with the physical parameters $E = 10^8$ and $\nu = 0.4999$. The computational domain is the rectangle $\Omega = (0, 5) \times (0, 1) \times (0, 1)$. The beam is clamped on one side, hence we consider the following problem

$$\begin{cases} -2\mu\nabla\cdot\boldsymbol{\varepsilon}(\boldsymbol{u}) + \nabla p = (0,0,-1)^T, & \text{in } \Omega, \\ -\nabla\cdot\boldsymbol{u} = \frac{1}{\lambda}p, & \text{in } \Omega, \\ \boldsymbol{u}(x,y) = (0,0,0)^T, & \text{on } \partial\Omega\cap\{x=0\}, \\ \boldsymbol{\sigma}_{\boldsymbol{n}}^{\text{sym}}(x,y) = (0,0,0)^T, & \text{on } \partial\Omega\setminus\{x=0\}. \end{cases}$$

TABLE 6.1
Comparison of preconditioners for Taylor-Hood discretisation ($\boldsymbol{TH}_{\boldsymbol{h}}^{\boldsymbol{2}}$, R_h^1)—the homogeneous beam.

		One-level					
DOF	N	ORAS	SORAS	NDTNS-MRAS	NDTNS-SMRAS	TDNNS-MRAS	TDNNS-SMRAS
32 446	8	21	45	29	36	27	37
73 548	16	31	70	38	64	26	67
139 794	32	43	99	74	94	66	91
299 433	64	55	143	161	140	149	139
549 396	128	78	192	314	192	229	199
		Two-level (6 eigenvectors)					
DOF	N	ORAS	SORAS	NDTNS-MRAS	NDTNS-SMRAS	TDNNS-MRAS	TDNNS-SMRAS
32 446	8	10	17	13	18	12	17
73 548	16	11	22	16	25	16	22
139 794	32	13	26	25	28	17	26
299 433	64	15	27	19	27	24	28
549 396	128	17	28	20	25	21	26
		Two-level (8 eigenvectors)					
DOF	N	ORAS	SORAS	NDTNS-MRAS	NDTNS-SMRAS	TDNNS-MRAS	TDNNS-SMRAS
32 446	8	9	16	12	17	12	16
73 548	16	10	19	15	24	14	20
139 794	32	11	21	17	23	17	21
299 433	64	14	24	17	24	21	23
549 396	128	16	27	18	23	20	22

The results of Table 6.1 show a clear improvement in the scalability of the two-level preconditioners over the one-level ones. In fact, using only zero energy modes, the number of iterations is virtually unaffected by the number of subdomains. All two-level preconditioners show a comparable performance. For this case, increasing the dimension of the coarse space beyond $6 \times N$ eigenvectors does not seem to improve the results significantly.

ETNA
Kent State University and
Johann Radon Institute (RICAM)

6.1.2. The Stokes equation. We now turn to the Stokes discrete problem given in Section 3.1. Once again, in the case of ORAS and SORAS we choose $\alpha = 10$ as in [16] for the Robin interface conditions (5.1).

TEST CASE 6.2 (The driven cavity problem). The test case is the three-dimensional version of the driven cavity problem. We consider the following problem on the unit cube $\Omega = (0,1)^3$

$$\begin{cases} -\Delta \boldsymbol{u} + \nabla p = \boldsymbol{f}, & \text{in } \Omega, \\ -\nabla \cdot \boldsymbol{u} = 0, & \text{in } \Omega, \\ \boldsymbol{u}(x,y) = (1,0,0)^T, & \text{on } \partial\Omega \cap \{y=1\}, \\ \boldsymbol{u}(x,y) = (0,0,0)^T, & \text{on } \partial\Omega \setminus \{y=1\}. \end{cases}$$

TABLE 6.2
Comparison of preconditioners for Taylor-Hood discretisation ($\boldsymbol{TH_h^2}, R_h^1$)—the driven cavity problem.

		One-level					
DOF	N	ORAS	SORAS	NVTF-MRAS	NVTF-SMRAS	TVNF-MRAS	TVNF-SMRAS
38 229	8	12	24	12	22	11	23
76 542	16	18	34	18	31	15	31
158 818	32	23	45	20	45	19	45
325 293	64	28	60	36	64	25	60
643 137	128	37	79	64	91	33	88
		Two-level (3 eigenvectors)					
DOF	N	ORAS	SORAS	NVTF-MRAS	NVTF-SMRAS	TVNF-MRAS	TVNF-SMRAS
38 229	8	10	17	10	18	11	18
76 542	16	11	20	11	19	14	19
158 818	32	13	24	13	24	16	23
325 293	64	15	27	15	27	19	26
643 137	128	18	31	17	32	22	31
		Two-level (7 eigenvectors)					
DOF	N	ORAS	SORAS	NVTF-MRAS	NVTF-SMRAS	TVNF-MRAS	TVNF-SMRAS
38 229	8	9	16	9	16	12	17
76 542	16	10	17	10	18	15	17
158 818	32	11	19	11	20	17	20
325 293	64	13	19	13	21	20	20
643 137	128	15	21	16	22	22	22

The conclusions remain the same as for the homogeneous beam example for the nearly incompressible elasticity equation discretised by Taylor-Hood method ($\boldsymbol{TH_h^3}, R_h^2$), since Tables 6.1 and 6.2 show similar results.

7. Conclusion. We tested numerically two-level preconditioners with spectral coarse spaces for nearly incompressible elasticity and Stokes equations. We considered two finite element methods, namely, Taylor-Hood (Section 3.1) and the hdG (Section 3.2) discretisations.

In the case of the homogeneous nearly incompressible elasticity the two-level methods coupled with the SORAS preconditioner, defined in [16], and the SMRAS preconditioner, defined by (4.2), allowed us to achieve good scalability results for both discretisations. Furthermore, for these symmetric preconditioners coarse spaces containing only zero energy modes seem to be sufficient for two and three dimensional problems. For the heterogeneous problem we also achieved scalability for two-level SORAS and SMRAS preconditioners, but, as expected, only in the case when the size of the coarse space is sufficiently large.

ETNA
Kent State University and
Johann Radon Institute (RICAM)

The improvement in convergence, in the case of the Stokes flow, is visible only when the coarse space contains more eigenvectors than only constants. For the Taylor-Hood discretisation, taking a sufficiently large coarse space we were able to achieve good scalability for all preconditioners. It is remarkable that these good results occur even when using the hdG discretisation, despite the fact that the optimized parameter to be used in SORAS and ORAS is not available.

We can conclude that the two-level preconditioners associated with non-standard interface conditions are at least as good as the two-level ones in conjunction with Robin interface conditions using optimised parameters. This shows an important advantage of the newly introduced preconditioners, as they are parameter-free. This allows a more flexible use of them, since they do not need a discretisation-based tuning. In fact, no change needs to be made in their implementation when changing from a continuous to a discontinuous discretisation.

Numerical tests have shown that the coarse spaces bring an important improvement in the convergence, but the size of the coarse space depends on the problem. Building as small as possible coarse spaces is important from a computational point of view. Thus, it is necessary to investigate what could be an optimal criterion for choosing the eigenvectors for a coarse space.

As the authors of [16] pointed out, an appropriate theory for obtaining a user-prescribed convergence rate when using spectral coarse spaces, in the same spirit as the one developed for SPD problems, remains an open problem and does not seem to be an easy task. The main theoretical arguments that apply for the latter, that is the Fictitious Space Lemma, cannot be extended easily to saddle point problems. Our purpose was then to limit the analysis of our preconditioner to numerical arguments by providing extensive results on different standard test cases.

Acknowledgements. The work by Michal Bosy was partially funded by the Engineering and Physical Sciences Research Council of Great Britain under the Numerical Algorithms and Intelligent Software (NAIS) for the evolving HPC platform grant EP/G036136/1. We thank Frédéric Nataf and Pierre-Henri Tournier for many helpful discussions and insightful comments, and Ryadh Haferssas and Frédéric Hecht for their assistance with the FreeFem++ codes.

REFERENCES

[1] H. ALCIN, B. KOOBUS, O. ALLAIN, AND A. DERVIEUX, *Efficiency and scalability of a two-level Schwarz algorithm for incompressible and compressible flows*, Internat. J. Numer. Methods Fluids, 72 (2013), pp. 69–89.

[2] B. AYUSO DE DIOS, F. BREZZI, L. D. MARINI, J. XU, AND L. ZIKATANOV, *A simple preconditioner for a discontinuous Galerkin method for the Stokes problem*, J. Sci. Comput., 58 (2014), pp. 517–547.

[3] G. R. BARRENECHEA, M. BOSY, V. DOLEAN, F. NATAF, AND P.-H. TOURNIER, *Hybrid discontinuous Galerkin discretisation and domain decomposition preconditioners for the Stokes problem*, Comput. Methods Appl. Math. (2018). Available online, DOI:10.1515/cmam-2018-0005.

[4] D. BOFFI, F. BREZZI, AND M. FORTIN, *Mixed Finite Element Methods and Applications*, Springer, Heidelberg, 2013.

[5] M. BREZINA, C. I. HEBERTON, J. MANDEL, AND P. VANEK, *An iterative method with convergence rate chosen a priori*, Tech. Rep. UCD/CCM Report 140, Center for Computational Mathematics, University of Colorado at Denver, Denver, 1999.

[6] C. CARSTENSEN AND M. SCHEDENSACK, *Medius analysis and comparison results for first-order finite element methods in linear elasticity*, IMA J. Numer. Anal., 35 (2015), pp. 1591–1621.

[7] B. COCKBURN AND J. GOPALAKRISHNAN, *The derivation of hybridizable discontinuous Galerkin methods for Stokes flow*, SIAM J. Numer. Anal., 47 (2009), pp. 1092–1125.

[8] B. COCKBURN, J. GOPALAKRISHNAN, AND R. LAZAROV, *Unified hybridization of discontinuous Galerkin, mixed, and continuous Galerkin methods for second order elliptic problems*, SIAM J. Numer. Anal., 47 (2009), pp. 1319–1365.

ETNA
Kent State University and
Johann Radon Institute (RICAM)

[9] L. CONEN, V. DOLEAN, R. KRAUSE, AND F. NATAF, *A coarse space for heterogeneous Helmholtz problems based on the Dirichlet-to-Neumann operator*, J. Comput. Appl. Math., 271 (2014), pp. 83–99.

[10] V. DOLEAN, P. JOLIVET, AND F. NATAF, *An Introduction to Domain Decomposition Methods*, SIAM, Philadelphia, 2015.

[11] V. DOLEAN, F. NATAF, R. SCHEICHL, AND N. SPILLANE, *Analysis of a two-level Schwarz method with coarse spaces based on local Dirichlet-to-Neumann maps*, Comput. Methods Appl. Math., 12 (2012), pp. 391–414.

[12] Y. EFENDIEV, J. GALVIS, R. LAZAROV, AND J. WILLEMS, *Robust domain decomposition preconditioners for abstract symmetric positive definite bilinear forms*, ESAIM Math. Model. Numer. Anal., 46 (2012), pp. 1175–1199.

[13] J. GALVIS AND Y. EFENDIEV, *Domain decomposition preconditioners for multiscale flows in high-contrast media*, Multiscale Model. Simul., 8 (2010), pp. 1461–1483.

[14] ———, *Domain decomposition preconditioners for multiscale flows in high contrast media: reduced dimension coarse spaces*, Multiscale Model. Simul., 8 (2010), pp. 1621–1644.

[15] V. GIRAULT AND P.-A. RAVIART, *Finite element methods for Navier-Stokes equations*, Springer, Berlin, 1986.

[16] R. HAFERSSAS, P. JOLIVET, AND F. NATAF, *An additive Schwarz method type theory for Lions's algorithm and a symmetrized optimized restricted additive Schwarz method*, SIAM J. Sci. Comput., 39 (2017), pp. A1345–A1365.

[17] F. HECHT, *New development in FreeFem++*, J. Numer. Math., 20 (2012), pp. 251–265.

[18] G. KARYPIS AND V. KUMAR, *METIS—A software package for partitioning unstructured graphs, partitioning meshes, and computing fill-reducing orderings of sparse matrices*, Tech. Rep., University of Minnesota, Department of Computer Science and Engineering, Army HPC Research Center, Minneapolis, 1998.

[19] A. KLAWONN AND L. F. PAVARINO, *Overlapping Schwarz methods for mixed linear elasticity and Stokes problems*, Comput. Methods Appl. Mech. Engrg., 165 (1998), pp. 233–245.

[20] R. B. LEHOUCQ, D. C. SORENSEN, AND C. YANG, *ARPACK users' guide*, SIAM, Philadelphia, 1998.

[21] S. LOISEL, H. NGUYEN, AND R. SCHEICHL, *Optimized Schwarz and 2-Lagrange multiplier methods for multiscale elliptic PDEs*, SIAM J. Sci. Comput., 37 (2015), pp. A2896–A2923.

[22] F. NATAF, H. XIANG, AND V. DOLEAN, *A two level domain decomposition preconditioner based on local Dirichlet-to-Neumann maps*, C. R. Math. Acad. Sci. Paris, 348 (2010), pp. 1163–1167.

[23] R. A. NICOLAIDES, *Deflation of conjugate gradients with applications to boundary value problems*, SIAM J. Numer. Anal., 24 (1987), pp. 355–365.

[24] A. PECHSTEIN AND J. SCHÖBERL, *Tangential-displacement and normal-normal-stress continuous mixed finite elements for elasticity*, Math. Models Methods Appl. Sci., 21 (2011), pp. 1761–1782.

[25] Y. SAAD AND M. H. SCHULTZ, *GMRES: a generalized minimal residual algorithm for solving nonsymmetric linear systems*, SIAM J. Sci. Statist. Comput., 7 (1986), pp. 856–869.

[26] N. SPILLANE, V. DOLEAN, P. HAURET, F. NATAF, C. PECHSTEIN, AND R. SCHEICHL, *Abstract robust coarse spaces for systems of PDEs via generalized eigenproblems in the overlaps*, Numer. Math., 126 (2014), pp. 741–770.

[27] A. TOSELLI AND O. WIDLUND, *Domain Decomposition Methods—Algorithms and Theory*, Springer, Berlin, 2005.